



# It Takes a Village: Multimodality Imaging of Cardiac Amyloidosis

REVIEW

JEAN MICHEL SAAD, MD

YUSHUI HAN, MS

AHMED IBRAHIM AHMED, MD, MPH

MOATH SAID ALFAWARA, MD

DIXITHA ANUGULA, MD

MOUAZ H. AL-MALLAH, MD, MSc

*\*Author affiliations can be found in the back matter of this article*

HOUSTON  
**Methodist**  
DEBAKEY HEART &  
VASCULAR CENTER

## ABSTRACT

Cardiac amyloidosis (CA) is the buildup and infiltration of amyloid plaque in cardiac muscle. An underdiagnosed form of restrictive cardiomyopathy, CA can rapidly progress into heart failure. CA is evaluated using a multimodality approach that includes echocardiography, cardiac magnetic imaging, and nuclear imaging. Echocardiography remains an essential first-line modality that raises suspicion for CA and establishes functional baselines. Cardiac magnetic imaging provides additional incremental value via high-resolution imaging, robust functional assessment, and superior tissue characterization, all of which enable a more comprehensive investigation of CA. Cardiac scintigraphy has eliminated the need for invasive diagnostic approaches and helps differentiate CA subtypes. Positron emission tomography is the first modality introducing targeted amyloid binding tracers that allow for precise burden quantification, early detection, and disease monitoring. In this review, we highlight the role of several cardiac imaging techniques in the evaluation of CA.

CORRESPONDING AUTHOR:

**Mouaz H. Al-Mallah, MD, MSc**

Houston Methodist DeBakey  
Heart & Vascular Center,  
Houston Methodist Hospital,  
Houston, Texas, US

[mal-mallah@houstonmethodist.org](mailto:mal-mallah@houstonmethodist.org)

KEYWORDS:

cardiac amyloidosis; cardiac  
magnetic resonance imaging;  
echocardiography; PET; positron  
emission tomography; cardiac  
scintigraphy; pyrophosphate

TO CITE THIS ARTICLE:

Saad JM, Ahmed AI, Anugula  
D, Han Y, Alfawara MS, Al-  
Mallah MH. It Takes a Village:  
Multimodality Imaging  
of Cardiac Amyloidosis.  
Methodist DeBakey Cardiovasc  
J. 2022;18(2):47-58. doi:  
10.14797/mdcvj.1072

## INTRODUCTION

Cardiac amyloidosis (CA) is a clinical condition in which one of more than 30 different precursor proteins with unstable tertiary structure misfolds and aggregates as insoluble amyloid fibrils and deposits in the extracellular space of the heart.<sup>1</sup> CA leads to restrictive cardiomyopathy that predominantly presents as right ventricular (RV) failure. The workup and assessment of cardiac amyloidosis have employed a wide range of multimodality imaging techniques, each offering unique insights (*Figure 1*). This review discusses the role of several cardiac imaging techniques—including echocardiography, cardiac magnetic imaging, cardiac scintigraphy, and positron emission tomography (PET)—in the workup of CA.

## ECHOCARDIOGRAPHY

From M-mode findings almost 40 years ago, echocardiography has become a standard in any diagnostic evaluation of cardiac amyloidosis.<sup>2</sup> Echocardiography's widespread availability, accessibility, and low cost make it the first noninvasive imaging modality used when investigating the suspicion of CA.<sup>3</sup> Although not sensitive or specific enough to confirm a diagnosis, echocardiography provides critical information regarding disease status, cardiac function, and follow-up in the setting of good image quality and a high index of suspicion.<sup>4-7</sup>

Cardiac amyloidosis develops following increased deposition and accumulation of amyloid fibrils specifically in the ventricular walls. These depositions translate into

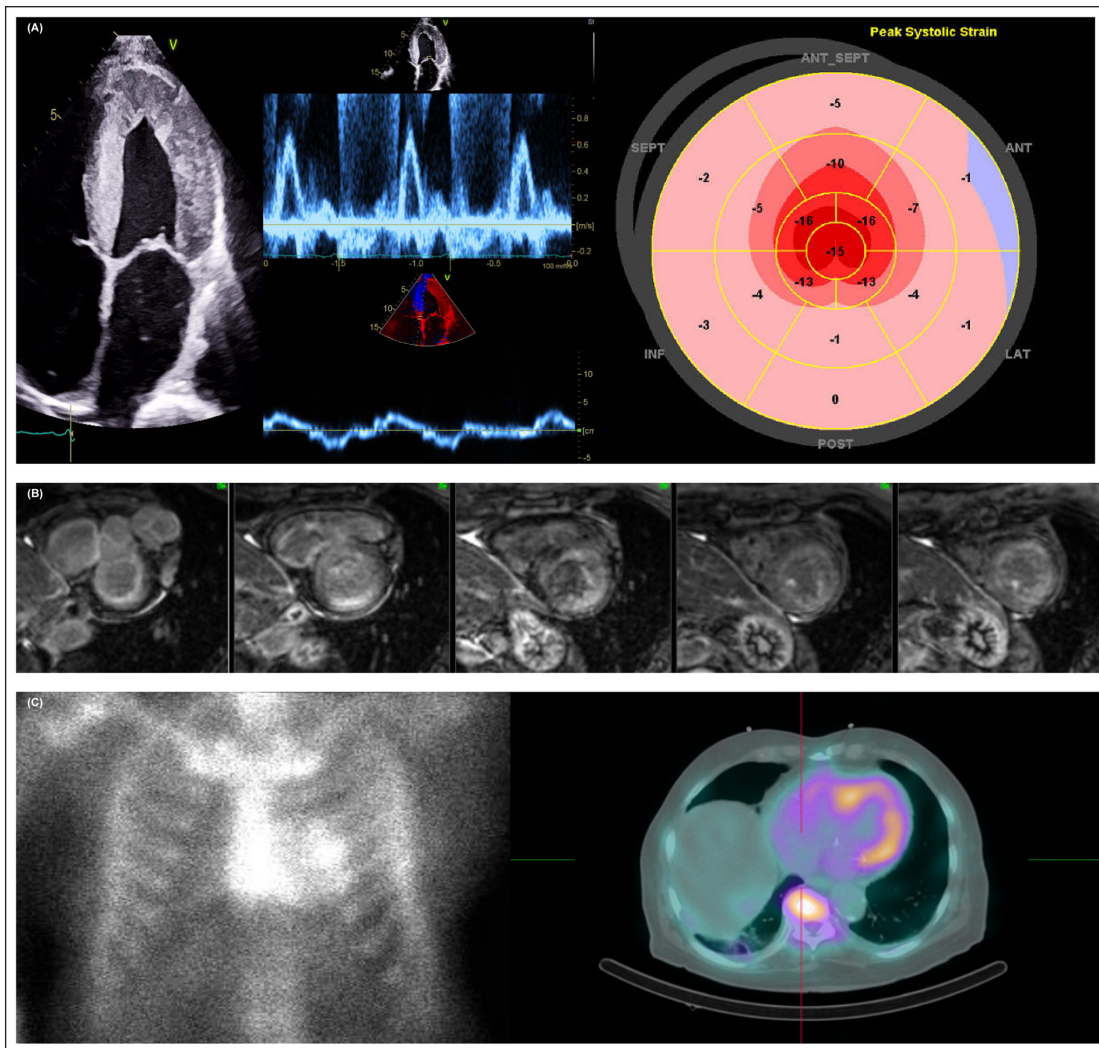


**Figure 1** Multimodality imaging approach for cardiac amyloidosis (CA). **(A)** Increased left ventricular (LV) wall and interatrial thickness with sparkling texture are typically found in patients with CA (left). Evidence of restrictive LV filling, rapid E-wave deceleration time, high E/A ratio on mitral inflow Doppler, and low myocardial relaxation velocities on tissue Doppler imaging (middle). Corresponding “bullseye” map of the longitudinal strain pattern of the LV with a “cherry on top” sign (right). **(B)** Cardiac magnetic resonance imaging shows characteristic imaging of CA with diffuse and subendocardial late gadolinium enhancement. **(C)** <sup>99m</sup>Tc-PYP anterior planar (left) imaging and single-photon emission computed tomography/computer tomography (right) showing a Perugini Grade of 2 and 3, respectively.

macro changes that form the basis of echocardiographic morphological assessment. These changes most prominently manifest as a thickened intraventricular septal wall > 12 mm that, in the absence of other causes of left ventricular (LV) hypertrophy, would indicate cardiac involvement in amyloid light-chain (AL) systemic amyloidosis.<sup>8</sup> However, the ability to accurately differentiate cardiac amyloidosis from other cardiomyopathies remains extremely difficult and highlights a recurrent limitation of echocardiography. Echocardiography can detect classical changes including thickening of the ventricular walls, interatrial septum, and valves, resulting in a smaller LV cavity, biatrial enlargement, and restrictive LV filling pattern.<sup>9-12</sup> Another reported finding includes a granular sparkling appearance of the myocardial wall, although this also was observed in other disease processes, namely end-stage renal disease.<sup>13</sup> More importantly, these changes are typically seen in more advanced stages of CA, hence limiting the utility of echocardiography in identifying early CA.

Echocardiography excels at providing exclusive insight into diastolic function and LV filling pressures. A high A-wave, low E-wave, and subsequently a reduced E/A ratio are indicative of possible early-stage CA compared with low A-wave and normal E-wave leading to a high E/A ratio in late CA.<sup>14</sup> Advanced restrictive patterns also include a rapid decelerating diastolic MV inflow time and small S-wave pulmonary venous spectral Doppler patterns. Furthermore, reduced mitral and tricuspid annular velocities and a high E/e' ratio are also indicative of increased filling pressures.<sup>15</sup>

Cardiac amyloidosis has exhibited a progressive pattern of diastolic dysfunction characterized by impaired relaxation. Following a stage of preserved ejection fraction,<sup>16,17</sup> these patterns ultimately lead to a deterioration of LV function.<sup>18</sup> Similar patterns are also noted using other functional assessment parameters such as stroke volume index and myocardial contraction fraction (MCF), which have both proven to be better diagnostic markers than ejection fraction.

Moreover, stroke volume index is easily obtained and prognostically useful in patients with AL-CA, making it an essential parameter in the CA workup.<sup>17</sup> MCF is a ratio of stroke volume to myocardial volume, thus creating an index that assesses volumetric shortening of the myocardium independent of chamber size and geometry.<sup>19-21</sup>

Although most conventional echocardiographic parameters report low diagnostic accuracy due to low sensitivity, other parameters have shown remarkable specificities. Some examples include E/e' ratio (> 9.6 specificity is 100%, and sensitivity 50%), left atrial volume index ( $\geq 47$  mL/m<sup>2</sup> specificity is 93%, and sensitivity 44%), and MCF ( $\leq 0.234$  specificity is 96%, and sensitivity 56%).<sup>22</sup>

The recent implementation of Doppler imaging and speckle-tracking echocardiography has introduced longitudinal strain measurement as a useful assessment of quantitative systolic function.<sup>11,23,24</sup> Using 2-dimensional (2D) speckle tracking, abnormal myocardial deformation has been detected in as many as 93% to 100% of patients with CA.<sup>11</sup>

Moreover, both transthyretin amyloidosis (ATTR) and AL cardiac amyloidosis are known to lead to reduced global longitudinal strain prior to any noticeable changes in left ventricular ejection fraction. However, this is more prominent in the detection of ATTR cardiomyopathy (ATTR-CA), with a global longitudinal strain of -15.1 or greater reporting an area under the curve (AUC) of 0.85 (87% sensitivity and 72% specificity).<sup>22</sup> Furthermore, a regional gradient pattern showing impairment of the mid and basal segments with relative sparing of the apex—known as the “bullseye”—is consistent with cardiac amyloidosis.<sup>25,26</sup> Although the underlying pathophysiology remains unclear, this pattern has allowed clinicians to differentiate between cardiac amyloidosis and other causes of LV hypertrophy, such as hypertensive cardiomyopathy or aortic stenosis, which typically present with reduced LV longitudinal strain in the areas of maximum hypertrophy.<sup>26,27</sup> An apical/average longitudinal strain ratio > 1.0 in the mid and basal segments was able to distinguish CA from LV hypertrophy (93% sensitivity, 82% specificity).<sup>26</sup> Reduced global longitudinal strain carries significant prognostic implications in both AL amyloidosis and ATTR.<sup>11,25,28</sup>

## CARDIAC MAGNETIC RESONANCE

Improved technology and heightened provider awareness have led to the increased use of cardiac magnetic imaging (CMR) in the workup of cardiac amyloidosis.<sup>29</sup> CMR provides additional incremental value in the form of high-resolution imaging, robust functional assessment, and superior tissue characterization, enabling a more comprehensive investigation of CA. The use of CMR is therefore crucial to the continued assessment of CA, especially in cases of poor acoustic windows or uncertain diagnosis following echocardiography. In addition to anatomical and functional assessment, CMR offers an array of other parameters in the workup of CA, including T1/T2-weighted imaging, T1/T2 mapping, late gadolinium enhancement (LGE), and extracellular volume (ECV).<sup>3</sup>

As previously noted on echocardiography, CA was known to cause LV hypertrophy across AL amyloidosis and ATTR-CA. However, owing to its high image resolution and 3D image acquisition, CMR noted that concentric symmetrical LV hypertrophy is more typical of AL amyloidosis, occurring in

approximately 79% of patients. Conversely, 68% of patients with ATTR-CA have asymmetrical hypertrophy compared with 18% of those with AL amyloidosis,<sup>30</sup> while no differences were noted among the subtypes of ATTR-CA: wild-type ATTR and hereditary ATTR. In addition, amyloid deposition in the RV wall results in a typical RV hypertrophy morphology.

Another unique advantage offered by CMR is LGE, a highly accurate finding for the detection of CA (*Figure 2*).<sup>31,32</sup> First described by Maceira et al., global subendocardial LGE became a pathognomonic finding highly suggestive of CA.<sup>31</sup> Furthermore, LGE in the left atrium is specific for differentiating cardiac amyloidosis from other hypertrophic cardiomyopathies.<sup>33</sup>

Initial implementation of LGE proved technically challenging due to difficulty with myocardial nulling. However, the use of a widely available phase-sensitive inversion recovery sequence (PSIR) helped resolve previous issues with optimal nulling settings and served to increase the reliability and application of LGE CMR.<sup>31</sup> LGE was also used to track progression in both AL and ATTR amyloidosis based on progression from typical subendocardial to transmural enhancement.<sup>34,35</sup> Although other LGE patterns were described, RV, subendocardial, and transmural remained the most commonly reported.<sup>30</sup> Studies comparing LGE patterns between ATTR and AL amyloidosis noted that while both forms exhibited similar LGE patterns, a higher prevalence of subendocardial LGE was reported in AL amyloidosis compared with transmural and RV LGE in ATTR amyloidosis.<sup>30,35-37</sup>

Although LGE is a qualitative indicator of CA, it lacks the ability to quantitatively measure amyloid infiltration due to the large heterogeneity in pattern and signal intensities. Furthermore, LGE utilization is limited in patients with renal impairment, a subsequent manifestation in amyloidosis patients.<sup>38</sup>

In contrast, T1 and ECV provide benchmarks to quantify and track disease burden, allowing for disease stratification and evaluation of response to therapy.<sup>39</sup> T1- and T2-weighted imaging sequences are intrinsic magnetic parameters based on the abundance and magnetization of hydrogen nuclei in tissues. Native (noncontrast) T1 mapping is a composite signal from both extra and intracellular spaces (*Figure 3*).<sup>40,41</sup> The addition of contrast (LGE) accentuates these properties and allows for the isolation and measurement of ECV, categorizing T1 mapping as precontrast (native T1) and postcontrast (ECV). Native myocardial T1 is a measurement of myocardial T1 relaxation times using noncontrast CMR, noting increased T1 values in both AL and ATTR amyloidosis.<sup>42</sup> Similar diagnostic accuracy for detecting ATTR amyloidosis was reported by Fontana et al., albeit with a lower T1 elevation compared with AL amyloidosis.<sup>43</sup> Studies have also suggested the use of native T1 as a marker of early cardiac involvement.<sup>42,43</sup>

Because amyloid deposition results in the gradual expansion of the extracellular matrix, the quantification of ECV can potentially provide insight into disease burden and degree of amyloid infiltration. Several studies reported an increase in ECV in both AL and ATTR amyloidosis.<sup>39-41</sup> More importantly, studies have shown how an increase in ECV can serve as an early marker of disease since it is identified before LGE and abnormal findings in other imaging modalities.<sup>44</sup>

Higher native myocardial T1 mapping was able to identify and stratify worse prognosis in AL-CA but not in ATTR-CA.<sup>45,46</sup> On the other hand, ECV has shown prognostic association in both AL and ATTR-CA. Ultimately, incremental to traditional risk factors, both LGE and ECV can serve as independent predictors of disease prognosis.<sup>30,45,47</sup>

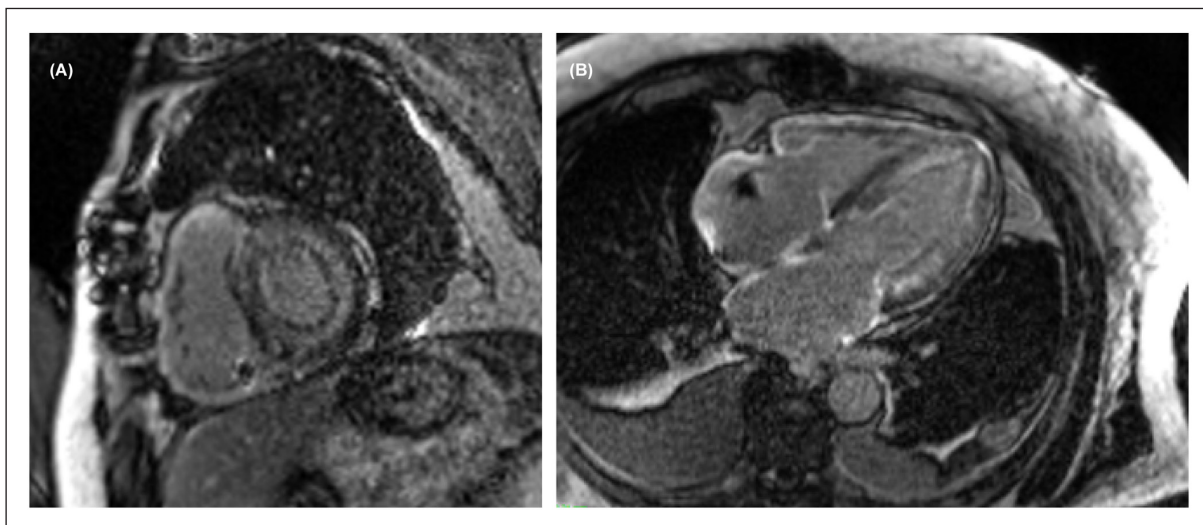


**Figure 2** (A) Short-axis view and (B) long-axis view shows diffuse late gadolinium enhancement uptake (Siemens 1.5 Tesla).

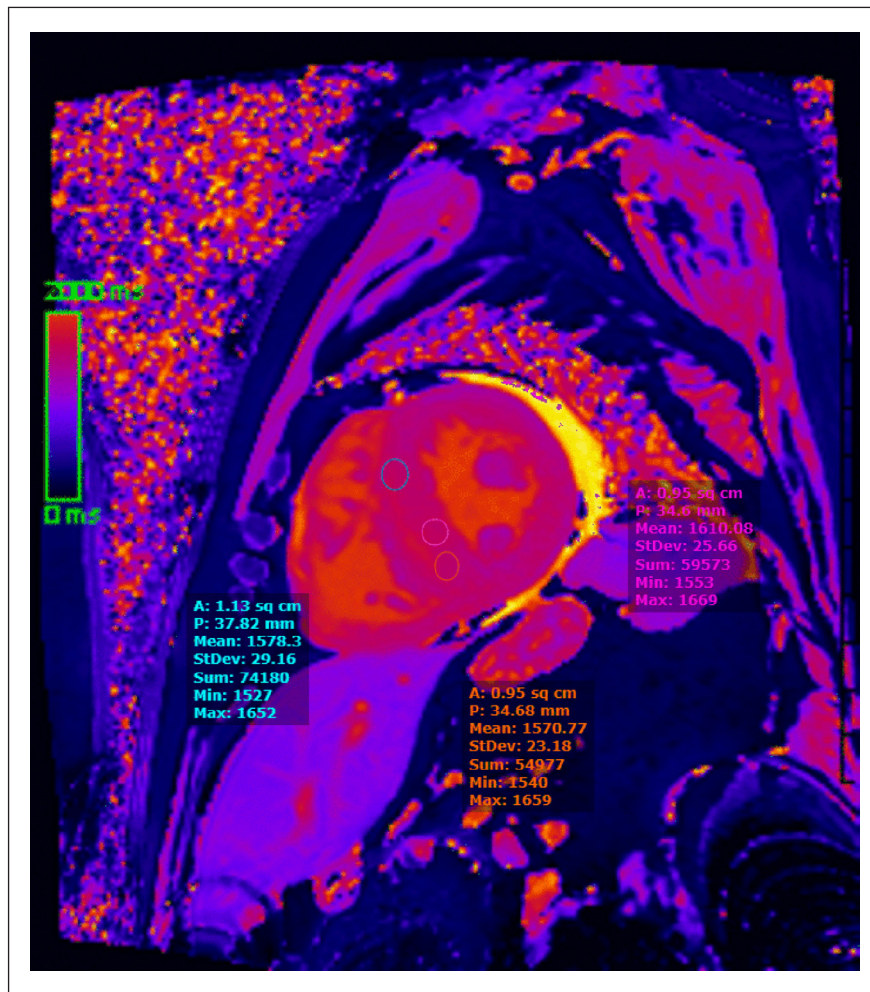


**Figure 3** T1 map (precontrast) shows the left ventricle with an elevation of native T1 values (Siemens 1.5 Tesla).

CMR myocardial T2 mapping provides another dimension of tissue characterization by visualizing and quantifying myocardial edema. Prior studies have revealed elevated T2/myocardial edema in patients with acute myocardial infarction, myocarditis, and heart failure.<sup>48,49</sup> Although T2 ratios in CA reported conflicting results, T2 mapping has shown consistent elevation in both ATTR and AL-CA. Furthermore, T2 was also shown to be an independent predictor of mortality even after adjusting for ECV and NT-proBNP.<sup>50</sup>

## TECHNETIUM-LABELED CARDIAC SCINTIGRAPHY

Cardiac scintigraphy provides incremental value in the workup of CA because it can differentiate between AL and ATTR amyloidosis.<sup>3,51</sup> More importantly, <sup>99m</sup>Tc-labeled radiotracer cardiac scintigraphy prevents the need for invasive diagnostic procedures in patients screened for monoclonal gammopathies, effectively rewriting previous

diagnostic approaches to CA, especially ATTR-CA.<sup>3,52</sup> Initial interest in <sup>99m</sup>Tc-labeled bone scans as an imaging tool for amyloidosis began during the 1970s and 1980s after studies reported diffuse myocardial uptake, particularly in the right and left ventricles of patients with CA.<sup>53-57</sup> However, the potential of cardiac scintigraphy was not fully realized until the last two decades, following reports of improved diagnostic accuracy for ATTR-CA.<sup>58-60</sup>

Two grading systems are used for radiotracer uptake in single-photon emission computed tomography (SPECT) imaging, offering a semiquantitative and quantitative approach to CA workup. Heart to contralateral lung (H/CL) was used to quantify uptake by comparing radiotracer retention, where an H/CL ratio > 1.5 was suggestive of ATTR-CA (**Figure 4**). Perugini et al. established a semiquantitative visual system to score planar images obtained at 3 hours post injection. This system was based on the uptake comparison between bone (rib) and the heart. The scoring system proposed was as follows: 0 = absent cardiac uptake, 1 = uptake less than bone, 2 = uptake equal to bone, and 3 = uptake greater than bone (**Figure 5**).<sup>58</sup>

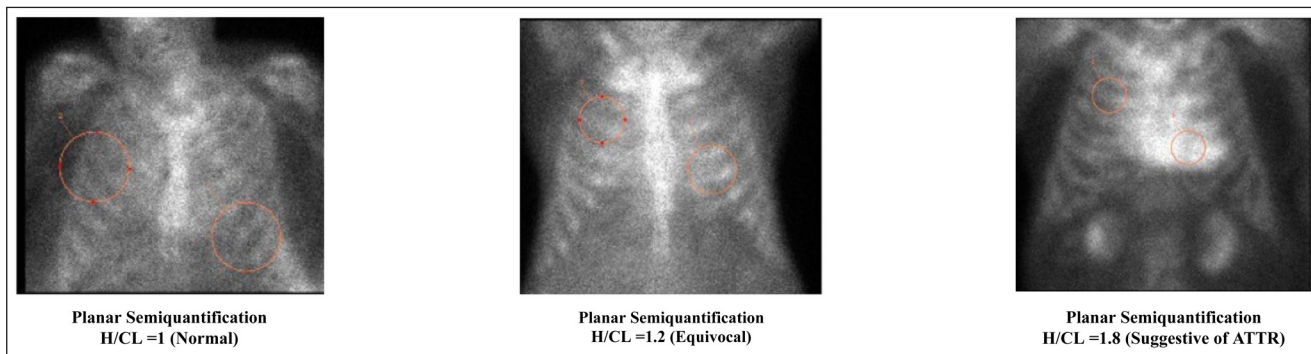


**Figure 4** <sup>99m</sup>Tc-PYP cardiac scintigraphy shows anterior planar imaging using heart-to-contralateral ratio semiquantitative scoring. Reproduced with permission from Springer Nature. doi: 10.1007/s10741-021-10174-x.

H/CL: heart to contralateral lung; ATTR: transthyretin amyloidosis

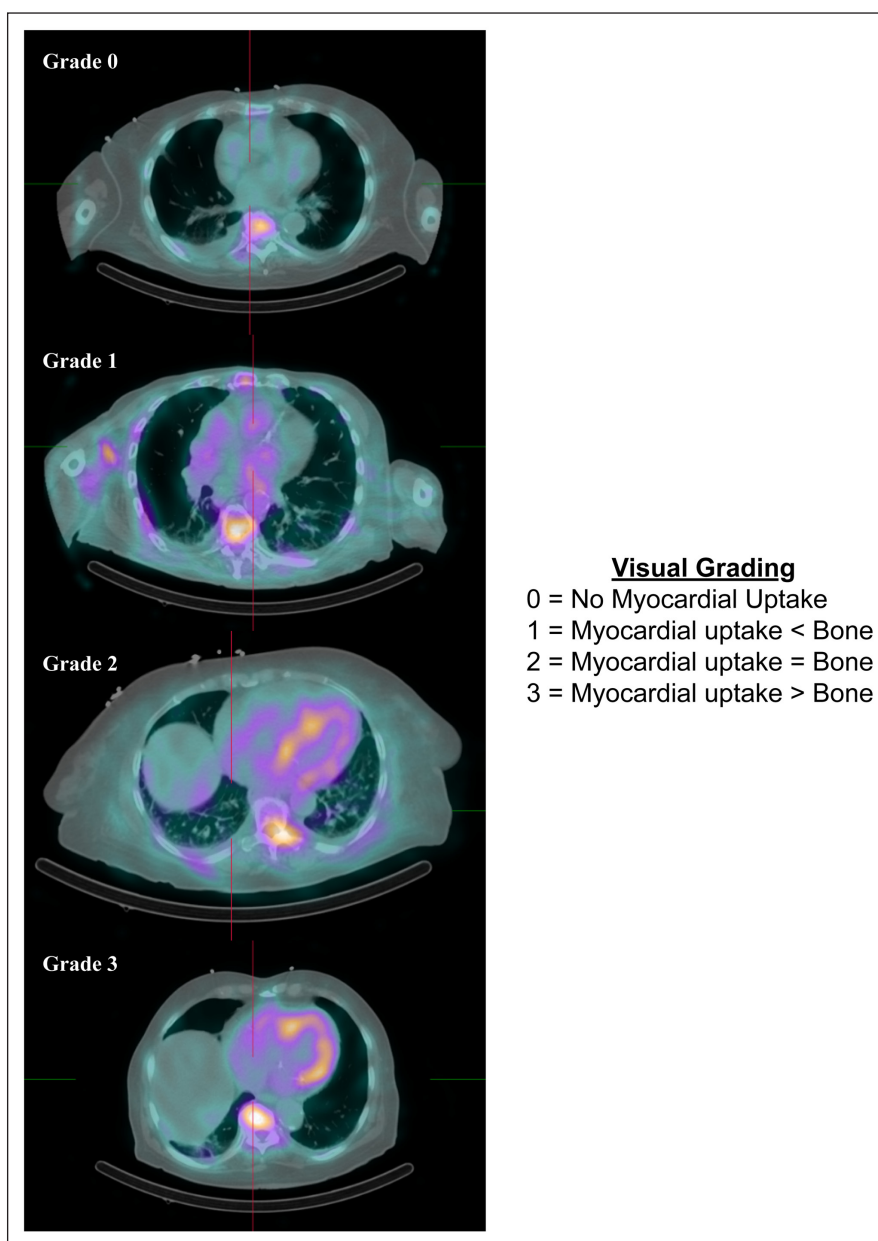


**Figure 5** <sup>99m</sup>Tc-PYP cardiac scintigraphy using single photo emission computer tomography/computed tomography visual scoring. Reproduced with permission from Springer Nature. doi: 10.1007/s10741-021-10174-x

Applying this visual scoring system revealed that any grade (1,2, or 3) conferred a sensitivity of > 99% but low specificity of 68% when compared with EMBs to identify ATTR. However, following the screening of patients for monoclonal gammopathy, a grade  $\geq 2$  established a sensitivity and specificity of 100% along with a 100% positive predictive value reproduced along all 3 radiotracers.<sup>52</sup> This obviated the need for more invasive confirmatory testing in patients with unexplained heart failure, suggestive echocardiography/CMR findings, and ruled out monoclonal gammopathy. Furthermore, a visual grade  $\geq 2$  also allowed the accurate differentiation of ATTR-CA from AL-CA (or unaffected controls). This is particularly relevant in the era of the new targeted amyloidosis treatments unique for both ATTR-CA and AL-CA.

The commonly investigated technetium-labeled radiotracers included <sup>99m</sup>Tc-pyrophosphate (<sup>99m</sup>Tc-PYP), <sup>99m</sup>Tc-3,3-diphosphono-1,2-propanodicarboxylic acid (<sup>99m</sup>Tc-DPD), <sup>99m</sup>Tc-hydroxymethylene diphosphonate (<sup>99m</sup>Tc-HMDP), and <sup>99m</sup>Tc methylene diphosphonate (<sup>99m</sup>Tc-MDP). <sup>99m</sup>Tc-PYP is commonly used in the United States (US), while <sup>99m</sup>Tc-DPD and <sup>99m</sup>Tc-HMDP are used in Europe. On the other hand, <sup>99m</sup>Tc-MDP, a widely available radiotracer in the US, is not routinely used due to its low sensitivity for detecting ATTR.<sup>61</sup>

It is also important to note that some specific hereditary ATTR mutations have shown varying uptakes and sensitivities in cardiac scintigraphy. In particular, V30M,<sup>62,63</sup> Y114C,<sup>63</sup> Thr59Lys,<sup>59</sup> and Phe64Leu<sup>64</sup> are reported as having low sensitivity with cardiac scintigraphy or no uptake with different Tc-labeled tracers (DPD and PYP) (**Table 1**). This discrepancy is due to specific TTR fibril compositions that include type A or type B (fragmented and full length versus exclusively full length, respectively),<sup>65,66</sup> with full-length fibrils exhibiting little to no radiotracer uptake. To prevent missed diagnoses, a high degree of suspicion and

a multimodality imaging approach are needed to balance out the inconsistencies presented by these mutations.

In addition to its diagnostic utility in the workup of CA, cardiac scintigraphy has also proven useful in some avenues of CA prognostication. Particularly, an H/CL ratio > 1.6 was shown to predict worse survival among patients with ATTR-CA.<sup>67</sup> Radiotracer retention grading and indices along different bone radiotracers have a reported association with cardiac biomarkers such as NT-proBNP, cardiac troponin T, and extracellular and other imaging parameters such as volume fraction, ejection fraction, LV wall thickness, and mass. Subsequently, radiotracer retention also has been associated with increased adverse cardiac outcomes such as advanced heart failure and mortality.<sup>67-71</sup>

## POSITRON EMISSION TOMOGRAPHY

Despite the attributes of cardiac scintigraphy, there continue to be gaps in the management of CA, such as the inability to clearly detect early disease as well as monitor disease progression and/or response to therapy. To counter these limitations, positron emission tomography (PET) has emerged as a new modality in the diagnostic evaluation of CA. PET offers several promising tracers such as Pittsburg Compound B, florbetapir, and florbetapan.<sup>72</sup> While these tracers were originally created to visualize and quantify beta-amyloid plaques in patients with Alzheimer's disease, they have since proven effective in diagnosing CA. Antoni et al. showed how there was a significant increase in <sup>11</sup>C-PiB (Pittsburgh Compound B) retention index (RI) in patients with ATTR-CA and AL-CA compared to controls.<sup>73</sup> A subsequent study showed significant differences in maximal and mean myocardium-to-blood cavity standard uptake value (SUV) ratios between AL-CA patients with

FALSE POSITIVE	FALSE NEGATIVE
Amyloid light-chain amyloidosis	Early disease
Hydroxychloroquine toxicity	Delayed imaging
Rib fracture	Full length (type B, Phe64Leu, Ser77Tyr, and Thr59Lys) transthyretin fibrils
Pleural effusion	Small radiotracer injection dose
Valvular calcification	Short acquisition time
Blood pool	Pericardial effusion
Breast implants	Breast implants
Myocardial infarction (acute or subacute)	
Rare forms of cardiac amyloidosis	
APO-A1 mutation	

**Table 1** Reported non-transthyretin amyloidosis causes of false positive and false negative Tc-labeled cardiac scintigraphy. Reproduced with permission from Springer Nature, doi: [10.1007/s10741-021-10174-x](https://doi.org/10.1007/s10741-021-10174-x)

prior chemotherapy versus chemotherapy naïve patients. This established the role of  $^{11}\text{C}$ -PiB as a surrogate indicator of active myocardial light chain deposition.<sup>74</sup> Rosengren et al. showed how CA without cardiac wall hypertrophy had increased  $^{11}\text{C}$ -PiB uptake, indicating a possible role in early diagnosis before the development of overt morphological changes.<sup>75</sup>

$^{18}\text{F}$ -florbetapir and  $^{18}\text{F}$ -florbetapan, PET tracers of the Stilbene class, could serve as molecular imaging biomarkers for CA as they bind directly to amyloid fibrils.<sup>76</sup> Earlier studies confirmed significant uptake of  $^{18}\text{F}$ -florbetapir in CA patients with a predilection for AL-CA compared to ATTR-CA.<sup>77</sup> Similarly,  $^{18}\text{F}$ -florbetapan has the potential to differentiate between non-CA, AL-CA, and ATTR-CA. Furthermore,  $^{18}\text{F}$ -florbetapan retention in CA was an independent determinant of functional and morphological parameters cardiac dysfunction on echocardiogram (for global LV longitudinal strain) and CMR imaging (for ventricular wall thickness).<sup>78,79</sup>

However, some new limitations arise with the use of these PET tracers—mainly, the shorter half-life of the  $^{11}\text{C}$ -PiB radiotracer versus  $^{18}\text{F}$ -labeled PET tracers. This necessitates the installation of an on-site cyclotron for continuous production, which may limit its accessibility and adoption.<sup>75</sup> Moreover, these radiotracers are not yet approved for clinical use and are only available in limited specialized centers.

PET imaging has brought forth new targeted amyloid-binding radiotracers that facilitate detection of all amyloid deposits regardless of the particular subtype of CA. More importantly, early studies have suggested that, using  $^{11}\text{C}$ -PiB and  $^{18}\text{F}$ -florbetapir, PET imaging may detect CA well before macroscopic changes such as wall thickening or later changes in cardiac biomarkers.<sup>75,80</sup> As such, PET introduces new avenues in the early diagnosis, monitoring, and assessment of CA burden.

## CONCLUSION

Multimodality imaging tools provide complementary roles in the diagnosis of patients with suspected CA. Echocardiography is the first-line test to identify nonspecific signs such as ventricular wall thickening and restrictive filling patterns. CMR enables high-resolution structural assessment as well as qualitative and quantitative measurement of amyloid infiltration. Pyrophosphate cardiac scintigraphy's strength is its ability to differentiate AL from ATTR amyloidosis. PET has an emerging role in early detection, disease monitoring, and response to therapy.

## KEY POINTS

- Cardiac amyloidosis (CA) remains an underdiagnosed cause of rapidly progressive heart failure. The evaluation of CA entails a multimodality imaging approach encompassing echocardiography, cardiac magnetic resonance (CMR), and nuclear imaging.
- The combination of echocardiography and CMR provides valuable anatomical and functional cardiac assessment in an effort to increase suspicion and maximize diagnostic accuracy.
- $^{99\text{m}}\text{Tc}$ -labeled radiotracer cardiac scintigraphy excels at differentiating and confirming the diagnosis of transthyretin CA following adequate screening and ruling out light-chain amyloidosis, obviating the need for more invasive biopsy approaches.
- The application of quantitative advanced cardiac imaging such as CMR and positron emission tomography have opened up new avenues in the early detection and prognostication of CA and tracking of therapeutic response, which is especially useful given the promising advancements in the treatment of CA.

## COMPETING INTERESTS

Dr. Mouaz Al-Mallah receives research support from Siemens unrelated to this study and is a consultant for Pfizer and Philips. All other authors have completed and submitted the *Methodist DeBakey Cardiovascular Journal* Conflict of Interest Statement and none were reported.

## AUTHOR AFFILIATIONS

**Jean Michel Saad, MD**  [orcid.org/0000-0002-8303-9415](https://orcid.org/0000-0002-8303-9415)

Houston Methodist DeBakey Heart & Vascular Center, Houston Methodist Hospital, Houston, Texas, US

**Ahmed Ibrahim Ahmed, MD, MPH**  [orcid.org/0000-0002-5886-7999](https://orcid.org/0000-0002-5886-7999)

Houston Methodist DeBakey Heart & Vascular Center, Houston Methodist Hospital, Houston, Texas, US

**Dixitha Anugula, MD**  [orcid.org/0000-0002-8571-2749](https://orcid.org/0000-0002-8571-2749)

Houston Methodist DeBakey Heart & Vascular Center, Houston Methodist Hospital, Houston, Texas, US

**Yushui Han, MS**  [orcid.org/0000-0002-8357-9729](https://orcid.org/0000-0002-8357-9729)

Houston Methodist DeBakey Heart & Vascular Center, Houston Methodist Hospital, Houston, Texas, US

**Moath Said Alfawara, MD**  [orcid.org/0000-0002-2676-3095](https://orcid.org/0000-0002-2676-3095)

Houston Methodist DeBakey Heart & Vascular Center, Houston Methodist Hospital, Houston, Texas, US

**Mouaz H. Al-Mallah, MD, MSc**  [orcid.org/0000-0003-2348-0484](https://orcid.org/0000-0003-2348-0484)

Houston Methodist DeBakey Heart & Vascular Center, Houston Methodist Hospital, Houston, Texas, US



## REFERENCES

1. **Arno S, Cowger J.** The genetics of cardiac amyloidosis. *Heart Fail Rev.* 2021 Sep 13. doi: [10.1007/s10741-021-10164-z](https://doi.org/10.1007/s10741-021-10164-z)
2. **Child JS, Levisman JA, Abbasi AS, MacAlpin RN.** Echocardiographic manifestations of infiltrative cardiomyopathy. A report of seven cases due to amyloid. *Chest.* 1976 Dec;70(6):726-31. doi: [10.1378/chest.70.6.726](https://doi.org/10.1378/chest.70.6.726)
3. **Dorbala S, Ando Y, Bokhari S, et al.** ASNC/AHA/ASE/EANM/HFSA/ISA/SCMR/SNMMI Expert Consensus Recommendations for Multimodality Imaging in Cardiac Amyloidosis: Part 1 of 2-Evidence Base and Standardized Methods of Imaging. *Circ Cardiovasc Imaging.* 2021 Jul;14(7):e000029. doi: [10.1161/HCI.000000000000029](https://doi.org/10.1161/HCI.000000000000029)
4. **Falk RH, Quarta CC.** Echocardiography in cardiac amyloidosis. *Heart Fail Rev.* 2015 Mar;20(2):125-31. doi: [10.1007/s10741-014-9466-3](https://doi.org/10.1007/s10741-014-9466-3)
5. **Falk RH, Alexander KM, Liao R, Dorbala S.** AL (Light-Chain) Cardiac Amyloidosis: A Review of Diagnosis and Therapy. *J Am Coll Cardiol.* 2016 Sep 20;68(12):1323-41. doi: [10.1016/j.jacc.2016.06.053](https://doi.org/10.1016/j.jacc.2016.06.053)
6. **Wechalekar AD, Gillmore JD, Hawkins PN.** Systemic amyloidosis. *Lancet.* 2016 Jun 25;387(10038):2641-2654. doi: [10.1016/S0140-6736\(15\)01274-X](https://doi.org/10.1016/S0140-6736(15)01274-X)
7. **Agrawal T, Nagueh SF.** Echocardiographic assessment of cardiac amyloidosis. *Heart Fail Rev.* 2021 Aug 30. doi: [10.1007/s10741-021-10165-y](https://doi.org/10.1007/s10741-021-10165-y)
8. **Gertz MA, Comenzo R, Falk RH, et al.** Definition of organ involvement and treatment response in immunoglobulin light chain amyloidosis (AL): a consensus opinion from the 10th International Symposium on Amyloid and Amyloidosis, Tours, France, 18-22 April 2004. *Am J Hematol.* 2005 Aug;79(4):319-28. doi: [10.1002/ajh.20381](https://doi.org/10.1002/ajh.20381)
9. **Nochioka K, Quarta CC, Claggett B, et al.** Left atrial structure and function in cardiac amyloidosis. *Eur Heart J Cardiovasc Imaging.* 2017 Oct 1;18(10):1128-1137. doi: [10.1093/ehjci/jex097](https://doi.org/10.1093/ehjci/jex097)
10. **Cueto-García L, Reeder GS, Kyle RA, et al.** Echocardiographic findings in systemic amyloidosis: spectrum of cardiac involvement and relation to survival. *J Am Coll Cardiol.* 1985 Oct;6(4):737-43. doi: [10.1016/s0735-1097\(85\)80475-7](https://doi.org/10.1016/s0735-1097(85)80475-7)
11. **Quarta CC, Solomon SD, Urazeer I, et al.** Left ventricular structure and function in transthyretin-related versus light-chain cardiac amyloidosis. *Circulation.* 2014 May 6;129(18):1840-9. doi: [10.1161/CIRCULATIONAHA.113.006242](https://doi.org/10.1161/CIRCULATIONAHA.113.006242)
12. **González-López E, Gagliardi C, Dominguez F, et al.** Clinical characteristics of wild-type transthyretin cardiac amyloidosis: disproving myths. *Eur Heart J.* 2017 Jun 21;38(24):1895-1904. doi: [10.1093/eurheartj/ehx043](https://doi.org/10.1093/eurheartj/ehx043)
13. **Habib G, Bucciarelli-Ducci C, Caforio ALP, et al.** Multimodality Imaging in Restrictive Cardiomyopathies: An EACVI expert consensus document In collaboration with the “Working Group on myocardial and pericardial diseases” of the European Society of Cardiology Endorsed by The Indian Academy of Echocardiography. *Eur Heart J Cardiovasc Imaging.* 2017 Oct 1;18(10):1090-1121. doi: [10.1093/ehjci/jex034](https://doi.org/10.1093/ehjci/jex034)
14. **Klein AL, Hatle LK, Burstow DJ, et al.** Doppler characterization of left ventricular diastolic function in cardiac amyloidosis. *J Am Coll Cardiol.* 1989 Apr;13(5):1017-26. doi: [10.1016/0735-1097\(89\)90254-4](https://doi.org/10.1016/0735-1097(89)90254-4)
15. **Koyama J, Ray-Sequin PA, Davidoff R, Falk RH.** Usefulness of pulsed tissue Doppler imaging for evaluating systolic and diastolic left ventricular function in patients with AL (primary) amyloidosis. *Am J Cardiol.* 2002 May 1;89(9):1067-71. doi: [10.1016/s0002-9149\(02\)02277-4](https://doi.org/10.1016/s0002-9149(02)02277-4)
16. **Austin BA, Duffy B, Tan C, Rodriguez ER, Starling RC, Desai MY.** Comparison of functional status, electrocardiographic, and echocardiographic parameters to mortality in endomyocardial-biopsy proven cardiac amyloidosis. *Am J Cardiol.* 2009 May 15;103(10):1429-33. doi: [10.1016/j.amjcard.2009.01.361](https://doi.org/10.1016/j.amjcard.2009.01.361)
17. **Knight DS, Giulia Z, William B, et al.** Cardiac Structural and Functional Consequences of Amyloid Deposition by Cardiac Magnetic Resonance and Echocardiography and Their Prognostic Roles. *JACC Cardiovasc Imaging.* 2019 May;12(5):823-833. doi: [10.1016/j.jcmg.2018.02.016](https://doi.org/10.1016/j.jcmg.2018.02.016)
18. **Tsang W, Lang RM.** Echocardiographic evaluation of cardiac amyloid. *Curr Cardiol Rep.* 2010 May;12(3):272-6. doi: [10.1007/s11886-010-0108-7](https://doi.org/10.1007/s11886-010-0108-7)
19. **Tendler A, Helmke S, Teruya S, Alvarez J, Maurer MS.** The myocardial contraction fraction is superior to ejection fraction in predicting survival in patients with AL cardiac amyloidosis. *Amyloid.* 2015 Mar;22(1):61-6. doi: [10.3109/13506129.2014.994202](https://doi.org/10.3109/13506129.2014.994202)
20. **Arenja N, Fritz T, Andre F, et al.** Myocardial contraction fraction derived from cardiovascular magnetic resonance cine images-reference values and performance in patients with heart failure and left ventricular hypertrophy. *Eur Heart J Cardiovasc Imaging.* 2017 Dec 1;18(12):1414-1422. doi: [10.1093/ehjci/jew324](https://doi.org/10.1093/ehjci/jew324)
21. **Milani P, Dispenzieri A, Scott CG, et al.** Independent Prognostic Value of Stroke Volume Index in Patients With Immunoglobulin Light Chain Amyloidosis. *Circ Cardiovasc Imaging.* 2018 May;11(5):e006588. doi: [10.1161/CIRCIMAGING.117.006588](https://doi.org/10.1161/CIRCIMAGING.117.006588)
22. **Pagourelías ED, Mirea O, Duchenne J, et al.** Echo Parameters for Differential Diagnosis in Cardiac Amyloidosis: A Head-to-Head Comparison of Deformation and Nondeformation Parameters. *Circ Cardiovasc Imaging.* 2017 Mar;10(3):e005588. doi: [10.1161/CIRCIMAGING.116.005588](https://doi.org/10.1161/CIRCIMAGING.116.005588)
23. **Buss SJ, Emami M, Mereles D, et al.** Longitudinal left ventricular function for prediction of survival in systemic

- light-chain amyloidosis: incremental value compared with clinical and biochemical markers. *J Am Coll Cardiol*. 2012 Sep 18;60(12):1067-76. doi: [10.1016/j.jacc.2012.04.043](https://doi.org/10.1016/j.jacc.2012.04.043)
24. **Koyama J, Ray-Sequin PA, Falk RH.** Longitudinal myocardial function assessed by tissue velocity, strain, and strain rate tissue Doppler echocardiography in patients with AL (primary) cardiac amyloidosis. *Circulation*. 2003 May 20;107(19):2446-52. doi: [10.1161/01.CIR.0000068313.67758.4F](https://doi.org/10.1161/01.CIR.0000068313.67758.4F)
  25. **Senapati A, Sperry BW, Grodin JL,** et al. Prognostic implication of relative regional strain ratio in cardiac amyloidosis. *Heart*. 2016 May 15;102(10):748-54. doi: [10.1136/heartjnl-2015-308657](https://doi.org/10.1136/heartjnl-2015-308657)
  26. **Phelan D, Collier P, Thavendiranathan P,** et al. Relative apical sparing of longitudinal strain using two-dimensional speckle-tracking echocardiography is both sensitive and specific for the diagnosis of cardiac amyloidosis. *Heart*. 2012 Oct;98(19):1442-8. doi: [10.1136/heartjnl-2012-302353](https://doi.org/10.1136/heartjnl-2012-302353)
  27. **Liu D, Hu K, Niemann M,** et al. Effect of combined systolic and diastolic functional parameter assessment for differentiation of cardiac amyloidosis from other causes of concentric left ventricular hypertrophy. *Circ Cardiovasc Imaging*. 2013 Nov;6(6):1066-72. doi: [10.1161/CIRCIMAGING.113.000683](https://doi.org/10.1161/CIRCIMAGING.113.000683)
  28. **Koyama J, Falk RH.** Prognostic significance of strain Doppler imaging in light-chain amyloidosis. *JACC Cardiovasc Imaging*. 2010 Apr;3(4):333-42. doi: [10.1016/j.jcmg.2009.11.013](https://doi.org/10.1016/j.jcmg.2009.11.013)
  29. **Pennell DJ.** Cardiovascular magnetic resonance: twenty-first century solutions in cardiology. *Clin Med (Lond)*. May-Jun 2003;3(3):273-8. doi: [10.7861/clinmedicine.3-3-273](https://doi.org/10.7861/clinmedicine.3-3-273)
  30. **Martinez-Naharro A, Treibel TA, Abdel-Gadir A,** et al. Magnetic Resonance in Transthyretin Cardiac Amyloidosis. *J Am Coll Cardiol*. 2017 Jul 25;70(4):466-477. doi: [10.1016/j.jacc.2017.05.053](https://doi.org/10.1016/j.jacc.2017.05.053)
  31. **Maceira AM, Joshi J, Prasad SK,** et al. Cardiovascular magnetic resonance in cardiac amyloidosis. *Circulation*. 2005 Jan 18;111(2):186-93. doi: [10.1161/01.CIR.0000152819.97857.9D](https://doi.org/10.1161/01.CIR.0000152819.97857.9D)
  32. **Fontana M, Chung R, Hawkins PN, Moon JC.** Cardiovascular magnetic resonance for amyloidosis. *Heart Fail Rev*. 2015 Mar;20(2):133-44. doi: [10.1007/s10741-014-9470-7](https://doi.org/10.1007/s10741-014-9470-7)
  33. **Kwong RY, Heydari B, Abbasi S,** et al. Characterization of Cardiac Amyloidosis by Atrial Late Gadolinium Enhancement Using Contrast-Enhanced Cardiac Magnetic Resonance Imaging and Correlation With Left Atrial Conduit and Contractile Function. *Am J Cardiol*. 2015 Aug 15;116(4):622-9. doi: [10.1016/j.amjcard.2015.05.021](https://doi.org/10.1016/j.amjcard.2015.05.021)
  34. **Fontana M, Treibel TA, Martinez-Naharro A,** et al. A case report in cardiovascular magnetic resonance: the contrast agent matters in amyloid. *BMC Med Imaging*. 2017 Jan 7;17(1):3. doi: [10.1186/s12880-016-0173-5](https://doi.org/10.1186/s12880-016-0173-5)
  35. **Fontana M, Pica S, Reant P,** et al. Prognostic Value of Late Gadolinium Enhancement Cardiovascular Magnetic Resonance in Cardiac Amyloidosis. *Circulation*. 2015 Oct 20;132(16):1570-9. doi: [10.1161/CIRCULATIONAHA.115.016567](https://doi.org/10.1161/CIRCULATIONAHA.115.016567)
  36. **Zhao L, Tian Z, Fang Q.** Diagnostic accuracy of cardiovascular magnetic resonance for patients with suspected cardiac amyloidosis: a systematic review and meta-analysis. *BMC Cardiovasc Disord*. 2016 Jun 7;16:129. doi: [10.1186/s12872-016-0311-6](https://doi.org/10.1186/s12872-016-0311-6)
  37. **Dungu JN, Valencia O, Pinney JH,** et al. CMR-based differentiation of AL and ATTR cardiac amyloidosis. *JACC Cardiovasc Imaging*. 2014 Feb;7(2):133-42. doi: [10.1016/j.jcmg.2013.08.015](https://doi.org/10.1016/j.jcmg.2013.08.015)
  38. **Bollée G, Guery B, Joly D,** et al. Presentation and outcome of patients with systemic amyloidosis undergoing dialysis. *Clin J Am Soc Nephrol*. 2008 Mar;3(2):375-81. doi: [10.2215/CJN.02470607](https://doi.org/10.2215/CJN.02470607)
  39. **Messroghli DR, Moon JC, Ferreira VM,** et al. Clinical recommendations for cardiovascular magnetic resonance mapping of T1, T2, T2\* and extracellular volume: A consensus statement by the Society for Cardiovascular Magnetic Resonance (SCMR) endorsed by the European Association for Cardiovascular Imaging (EACVI). *J Cardiovasc Magn Reson*. 2017 Oct 9;19(1):75. doi: [10.1186/s12968-017-0389-8](https://doi.org/10.1186/s12968-017-0389-8)
  40. **Moon JC, Messroghli DR, Kellman P,** et al. Myocardial T1 mapping and extracellular volume quantification: a Society for Cardiovascular Magnetic Resonance (SCMR) and CMR Working Group of the European Society of Cardiology consensus statement. *J Cardiovasc Magn Reson*. 2013 Oct 14;15(1):92. doi: [10.1186/1532-429X-15-92](https://doi.org/10.1186/1532-429X-15-92)
  41. **Banyersad SM, Sado DM, Flett AS,** et al. Quantification of myocardial extracellular volume fraction in systemic AL amyloidosis: an equilibrium contrast cardiovascular magnetic resonance study. *Circ Cardiovasc Imaging*. 2013 Jan 1;6(1):34-9. doi: [10.1161/CIRCIMAGING.112.978627](https://doi.org/10.1161/CIRCIMAGING.112.978627)
  42. **Karamitsos TD, Piechnik SK, Banyersad SM,** et al. Noncontrast T1 mapping for the diagnosis of cardiac amyloidosis. *JACC Cardiovasc Imaging*. 2013 Apr;6(4):488-97. doi: [10.1016/j.jcmg.2012.11.013](https://doi.org/10.1016/j.jcmg.2012.11.013)
  43. **Fontana M, Banyersad SM, Treibel TA,** et al. Native T1 mapping in transthyretin amyloidosis. *JACC Cardiovasc Imaging*. 2014 Feb;7(2):157-65. doi: [10.1016/j.jcmg.2013.10.008](https://doi.org/10.1016/j.jcmg.2013.10.008)
  44. **Martinez-Naharro A, Abdel-Gadir A, Treibel TA,** et al. CMR-Verified Regression of Cardiac AL Amyloid After Chemotherapy. *JACC Cardiovasc Imaging*. 2018 Jan;11(1):152-154. doi: [10.1016/j.jcmg.2017.02.012](https://doi.org/10.1016/j.jcmg.2017.02.012)
  45. **Banyersad SM, Fontana M, Maestrini V,** et al. T1 mapping and survival in systemic light-chain amyloidosis. *Eur Heart J*. 2015 Jan 21;36(4):244-51. doi: [10.1093/eurheartj/ehu444](https://doi.org/10.1093/eurheartj/ehu444)

46. **Martinez-Naharro A, Kotecha T, Norrington K**, et al. Native T1 and extracellular volume in transthyretin amyloidosis. *JACC Cardiovasc Imaging*. 2019 May;12(5):810-819. doi: [10.1016/j.jcmg.2018.02.006](https://doi.org/10.1016/j.jcmg.2018.02.006)
47. **Raina S, Lensing SY, Nairooz RS**, et al. Prognostic Value of Late Gadolinium Enhancement CMR in Systemic Amyloidosis. *JACC Cardiovasc Imaging*. 2016 Nov;9(11):1267-1277. doi: [10.1016/j.jcmg.2016.01.036](https://doi.org/10.1016/j.jcmg.2016.01.036)
48. **Legou F, Tacher V, Damy T**, et al. Usefulness of T2 ratio in the diagnosis and prognosis of cardiac amyloidosis using cardiac MR imaging. *Diagn Interv Imaging*. 2017 Feb;98(2):125-132. doi: [10.1016/j.diii.2016.08.007](https://doi.org/10.1016/j.diii.2016.08.007)
49. **Wassmuth R, Abdel-Aty H, Bohl S, Schulz-Menger J**. Prognostic impact of T2-weighted CMR imaging for cardiac amyloidosis. *Eur Radiol*. 2011 Aug;21(8):1643-50. doi: [10.1007/s00330-011-2109-3](https://doi.org/10.1007/s00330-011-2109-3)
50. **Kotecha T, Martinez-Naharro A, Treibel TA**, et al. Myocardial Edema and Prognosis in Amyloidosis. *J Am Coll Cardiol*. 2018 Jun 26;71(25):2919-2931. doi: [10.1016/j.jacc.2018.03.536](https://doi.org/10.1016/j.jacc.2018.03.536)
51. **Saad JM, Ahmed AI, Han Y, Saeed S, Pournazari P, Al-Mallah MH**. 99m Technetium-labeled cardiac scintigraphy for suspected amyloidosis: a review of current and future directions. *Heart Fail Rev*. 2021 Oct 28. doi: [10.1007/s10741-021-10174-x](https://doi.org/10.1007/s10741-021-10174-x)
52. **Gillmore JD, Maurer MS, Falk RH**, et al. Nonbiopsy Diagnosis of Cardiac Transthyretin Amyloidosis. *Circulation*. 2016 Jun 14;133(24):2404-12. doi: [10.1161/CIRCULATIONAHA.116.021612](https://doi.org/10.1161/CIRCULATIONAHA.116.021612)
53. **Ali A, Turner DA, Rosenbush SW, Fordham EW**. Bone scintigram in cardiac amyloidosis: a case report. *Clin Nucl Med*. 1981 Mar;6(3):105-8. doi: [10.1097/00003072-198103000-00003](https://doi.org/10.1097/00003072-198103000-00003)
54. **Sobol SM, Brown JM, Bunker SR, Patel J, Lull RJ**. Noninvasive diagnosis of cardiac amyloidosis by technetium-99m-pyrophosphate myocardial scintigraphy. *Am Heart J*. 1982 Apr;103(4 Pt 1):563-6. doi: [10.1016/0002-8703\(82\)90344-1](https://doi.org/10.1016/0002-8703(82)90344-1)
55. **Shih WJ, DeLand FH, Domstad PA, Stahr BJ, Powell RD, Yoneda K**. Scintigraphic findings in primary amyloidosis of the heart and stomach. *Clin Nucl Med*. 1985 Jul;10(7):466-7. doi: [10.1097/00003072-198507000-00003](https://doi.org/10.1097/00003072-198507000-00003)
56. **Li CK, Rabinovitch MA, Juni JE**, et al. Scintigraphic characterization of amyloid cardiomyopathy. *Clin Nucl Med*. 1985 Mar;10(3):156-9. doi: [10.1097/00003072-198503000-00004](https://doi.org/10.1097/00003072-198503000-00004)
57. **Janssen S, van Rijswijk MH, Piers DA, de Jong GM**. Soft-tissue uptake of 99mTc-diphosphonate in systemic AL amyloidosis. *Eur J Nucl Med*. 1984;9(12):538-41. doi: [10.1007/BF00256851](https://doi.org/10.1007/BF00256851)
58. **Perugini E, Guidalotti PL, Salvi F**, et al. Noninvasive etiologic diagnosis of cardiac amyloidosis using 99mTc-3,3-diphosphono-1,2-propanodicarboxylic acid scintigraphy. *J Am Coll Cardiol*. 2005 Sep 20;46(6):1076-84. doi: [10.1016/j.jacc.2005.05.073](https://doi.org/10.1016/j.jacc.2005.05.073)
59. **Bokhari S, Castaño A, Pozniakoff T, Deslisle S, Latif F, Maurer MS**. (99m)Tc-pyrophosphate scintigraphy for differentiating light-chain cardiac amyloidosis from the transthyretin-related familial and senile cardiac amyloidosis. *Circ Cardiovasc Imaging*. 2013 Mar 1;6(2):195-201. doi: [10.1161/CIRCIMAGING.112.000132](https://doi.org/10.1161/CIRCIMAGING.112.000132)
60. **Galat A, Rosso J, Guellich A**, et al. Usefulness of (99m)Tc-HMDP scintigraphy for the etiologic diagnosis and prognosis of cardiac amyloidosis. *Amyloid*. 2015;22(4):210-20. doi: [10.3109/13506129.2015.1072089](https://doi.org/10.3109/13506129.2015.1072089)
61. **Rapezzi C, Gagliardi C, Milandri A**. Analogies and disparities among scintigraphic bone tracers in the diagnosis of cardiac and non-cardiac ATTR amyloidosis. *J Nucl Cardiol*. 2019 Oct;26(5):1638-1641. doi: [10.1007/s12350-018-1235-6](https://doi.org/10.1007/s12350-018-1235-6)
62. **Coutinho MCA, Cortez-Dias N, Cantinho G**, et al. The sensitivity of DPD scintigraphy to detect transthyretin cardiac amyloidosis in V30M mutation depends on the phenotypic expression of the disease. *Amyloid*. 2020 Sep;27(3):174-183. doi: [10.1080/13506129.2020.1744553](https://doi.org/10.1080/13506129.2020.1744553)
63. **Pilebro B, Suhr OB, Näslund U, Westermark P, Lindqvist P, Sundström T**. (99m)Tc-DPD uptake reflects amyloid fibril composition in hereditary transthyretin amyloidosis. *Ups J Med Sci*. 2016;121(1):17-24. doi: [10.3109/03009734.2015.1122687](https://doi.org/10.3109/03009734.2015.1122687)
64. **Musumeci MB, Cappelli F, Russo D**, et al. Low Sensitivity of Bone Scintigraphy in Detecting Phe64Leu Mutation-Related Transthyretin Cardiac Amyloidosis. *JACC Cardiovasc Imaging*. 2020 Jun;13(6):1314-1321. doi: [10.1016/j.jcmg.2019.10.015](https://doi.org/10.1016/j.jcmg.2019.10.015)
65. **Takasone K, Katoh N, Takahashi Y**, et al. Non-invasive detection and differentiation of cardiac amyloidosis using 99m Tc-pyrophosphate scintigraphy and 11 C-Pittsburgh compound B PET imaging. *Amyloid*. 2020 Dec;27(4):266-274. doi: [10.1080/13506129.2020.1798223](https://doi.org/10.1080/13506129.2020.1798223)
66. **Pilebro B, Arvidsson S, Lindqvist P**, et al. Positron emission tomography (PET) utilizing Pittsburgh compound B (PIB) for detection of amyloid heart deposits in hereditary transthyretin amyloidosis (ATTR). *J Nucl Cardiol*. 2018 Feb;25(1):240-248. doi: [10.1007/s12350-016-0638-5](https://doi.org/10.1007/s12350-016-0638-5)
67. **Castano A, Haq M, Narotsky DL**, et al. Multicenter Study of Planar Technetium 99m Pyrophosphate Cardiac Imaging: Predicting Survival for Patients With ATTR Cardiac Amyloidosis. *JAMA Cardiol*. 2016 Nov 1;1(8):880-889. doi: [10.1001/jamacardio.2016.2839](https://doi.org/10.1001/jamacardio.2016.2839)
68. **Hutt DF, Fontana M, Burniston M**, et al. Prognostic utility of the Perugini grading of 99mTc-DPD scintigraphy in transthyretin (ATTR) amyloidosis and its relationship with skeletal muscle and soft tissue amyloid. *Eur Heart J Cardiovasc Imaging*. 2017 Dec 1;18(12):1344-1350. doi: [10.1093/ehjci/jew325](https://doi.org/10.1093/ehjci/jew325)

69. **Rapezzi C, Quarta CC, Guidalotti PL**, et al. Role of (99m) Tc-DPD scintigraphy in diagnosis and prognosis of hereditary transthyretin-related cardiac amyloidosis. *JACC Cardiovasc Imaging*. 2011 Jun;4(6):659-70. doi: [10.1016/j.jcmg.2011.03.016](https://doi.org/10.1016/j.jcmg.2011.03.016)
70. **Vranian MN, Sperry BW, Hanna M**, et al. Technetium pyrophosphate uptake in transthyretin cardiac amyloidosis: Associations with echocardiographic disease severity and outcomes. *J Nucl Cardiol*. 2018 Aug;25(4):1247-1256. doi: [10.1007/s12350-016-0768-9](https://doi.org/10.1007/s12350-016-0768-9)
71. **Sperry BW, Sato K, Phelan D**, et al. Regional Variability in Longitudinal Strain Across Vendors in Patients With Cardiomyopathy Due to Increased Left Ventricular Wall Thickness. *Circ Cardiovasc Imaging*. 2019 Aug;12(8):e008973. doi: [10.1161/CIRCIMAGING.119.008973](https://doi.org/10.1161/CIRCIMAGING.119.008973)
72. **Saeed S, Saad JM, Ahmed AI, Han Y, Al-Mallah MH**. The utility of positron emission tomography in cardiac amyloidosis. *Heart Fail Rev*. 2021 Nov 7. doi: [10.1007/s10741-021-10183-w](https://doi.org/10.1007/s10741-021-10183-w)
73. **Antoni G, Lubberink M, Estrada S**, et al. In vivo visualization of amyloid deposits in the heart with 11C-PIB and PET. *J Nucl Med*. 2013 Feb;54(2):213-20. doi: [10.2967/jnumed.111.102053](https://doi.org/10.2967/jnumed.111.102053)
74. **Lee S, Lee ES, Choi H**, et al. 11C-Pittsburgh B PET imaging in cardiac amyloidosis. *JACC Cardiovasc Imaging*. 2015 Jan;8(1):50-59. doi: [10.1016/j.jcmg.2014.09.018](https://doi.org/10.1016/j.jcmg.2014.09.018)
75. **Rosengren S, Skibsted Clemmensen T, Tolbod L**, et al. Diagnostic Accuracy of [11 C]PIB Positron Emission Tomography for Detection of Cardiac Amyloidosis. *JACC Cardiovasc Imaging*. 2020 Jun;13(6):1337-1347. doi: [10.1016/j.jcmg.2020.02.023](https://doi.org/10.1016/j.jcmg.2020.02.023)
76. **Choi SR, Schneider JA, Bennett DA**, et al. Correlation of amyloid PET ligand florbetapir F 18 binding with A aggregation and neuritic plaque deposition in postmortem brain tissue. *Alzheimer Dis Assoc Disord*. Jan-Mar 2012;26(1):8-16. doi: [10.1097/WAD.0b013e31821300bc](https://doi.org/10.1097/WAD.0b013e31821300bc)
77. **Park M, Padera RF, Belanger A**, et al. 18F-Florbetapir Binds Specifically to Myocardial Light Chain and Transthyretin Amyloid Deposits: Autoradiography Study. *Circ Cardiovasc Imaging*. 2015 Aug;8(8):10.1161/CIRCIMAGING.114.002954 e002954. doi: [10.1161/CIRCIMAGING.114.002954](https://doi.org/10.1161/CIRCIMAGING.114.002954)
78. **Law WP, Wang WYS, Moore PT, Mollee PN, Ng ACT**. Cardiac Amyloid Imaging with 18F-Florbetaben PET: A Pilot Study. *J Nucl Med*. 2016 Nov;57(11):1733-1739. doi: [10.2967/jnumed.115.169870](https://doi.org/10.2967/jnumed.115.169870)
79. **Kircher M, Ihne S, Brumberg J**, et al. Detection of cardiac amyloidosis with 18 F-Florbetaben-PET/CT in comparison to echocardiography, cardiac MRI and DPD-scintigraphy. *Eur J Nucl Med Mol Imaging*. 2019 Jul;46(7):1407-1416. doi: [10.1007/s00259-019-04290-y](https://doi.org/10.1007/s00259-019-04290-y)
80. **Cuddy SAM, Bravo PE, Falk RH**, et al. Improved Quantification of Cardiac Amyloid Burden in Systemic Light Chain Amyloidosis: Redefining Early Disease? *JACC Cardiovasc Imaging*. 2020 Jun;13(6):1325-1336. doi: [10.1016/j.jcmg.2020.02.025](https://doi.org/10.1016/j.jcmg.2020.02.025)

---

**TO CITE THIS ARTICLE:**

Saad JM, Ahmed AI, Anugula D, Han Y, Alfawara MS, Al-Mallah MH. It Takes a Village: Multimodality Imaging of Cardiac Amyloidosis. *Methodist DeBakey Cardiovasc J*. 2022;18(2):47-58. doi: [10.14797/mdcvj.1072](https://doi.org/10.14797/mdcvj.1072)

Submitted: 15 December 2021   Accepted: 17 January 2022   Published: 14 March 2022

**COPYRIGHT:**

© 2022 The Author(s). This is an open-access article distributed under the terms of the Attribution-NonCommercial 4.0 International (CC BY-NC 4.0), which permits unrestricted use, distribution, and reproduction in any noncommercial medium, provided the original author and source are credited. See <https://creativecommons.org/licenses/by-nc/4.0/>.

*Methodist DeBakey Cardiovascular Journal* is a peer-reviewed open access journal published by Houston Methodist DeBakey Heart & Vascular Center.